Experimental Evaluation on Lateral Torsional Buckling Resistance of Continuous Steel Stringers

C. Shawn Sun, Daniel G. Linzell, Jay A. Puckett, and Ahmed Rageh

ABSTRACT

An extensive experimental study evaluated lateral torsional buckling resistance of two-span, continuous, steel beams in a test assembly that included three beam lines, an interior transverse support (floor beam), and transverse diaphragms at the end supports. Funded by the Louisiana Transportation Research Center (LTRC), this study was conducted to better understand continuous stringer behavior so that simplified analyses would better capture their lateral torsional buckling (LTB) behavior. Current practice produces Louisiana Department of Transportation and Development (LA DOTD) bridge ratings often conservatively controlled by stringer LTB capacity and, in many cases, necessitates posting—thereby imposing significant and often unnecessary operational restrictions. Forty-seven elastic tests were completed. The tests encompassed a variety of unbraced lengths and support conditions with steel diaphragms or timber ties acting as bracing members. The interior beam in the test assembly was loaded orthogonal to its strong axis at the middle of one or both spans using a spreader beam that minimized restraint and prevented the development of follower forces. Tests demonstrated that minimal bracing could significantly increase lateral torsional buckling resistance and justify a higher LTB resistance than what is currently used. Although the tests were conducted on assemblies used to represent a bridge floor system, the results provided an extensive set of valuable data that could be used by structural steel researchers interested in examining flexural resistance of continuous beams.

Keywords: continuous, stringers, lateral torsional buckling, bracing.

INTRODUCTION

Some of Louisiana's bridges built in the 1950s and 1960s used two-girder or truss systems, in which floor beams are supported by main longitudinal members that then support continuous stringers (Figure 1). When the continuous stringers are load-rated, lateral torsional buckling (LTB) resistance is calculated in accordance with the *AASHTO LRFD Bridge Design Specifications* (AASHTO BDS) (AASHTO, 2020), which does not attempt to account for bracing effects that could be provided by a noncomposite deck. Consequently, LTB resistance can be underestimated and may necessitate load restrictions via unnecessarily conservative postings (Sun et al., 2021). This study, funded by the Louisiana Transportation Research Center (LTRC), was conducted to explore the development of more realistic replication of actual LTB resistance for continuous stringers supported by transverse floor beams. This paper presents the first set of tests of a reduced-scale assembly, those completed before placement of a noncomposite concrete deck, whose focus was examining LTB behavior of an interior, longitudinal stringer. These tests are generally applicable to LTB of any continuous steel beam, and the extensive amount of test results that were generated should be of interest to the steel research community.

C. Shawn Sun, Ph.D., PE, Assistant Professor, Department of Civil Engineering and Construction Management, California State University, Northridge, Calif. Email: shawn.sun@csun.edu (corresponding)

Daniel G. Linzell, Ph.D., PE, F.ASCE, F.SEI, Associate Dean and Leslie D. Martin Professor, Department of Civil and Environmental Engineering, University of Nebraska-Lincoln, Lincoln, Neb. Email: dlinzell@unl.edu

Jay A. Puckett, Ph.D., PE, F.ASCE, Professor, Durham School of Architectural Engineering and Construction, University of Nebraska-Lincoln, Omaha, Neb. Email: Jay.Puckett@unl.edu

Ahmed Rageh, Ph.D., Project Engineer, SDR Engineering, Tallahassee, Fla. Email: a.eissa.rageh@gmail.com

Paper No. 2021-08R

EXPERIMENTAL PROGRAM

As stated earlier, this paper summarizes an experimental program examining LTB resistance of two-span, continuous, steel stringers in a test assembly. The test assembly had three beam lines, an interior transverse support, and transverse diaphragms at its end supports. Forty-seven elastic tests were completed. The tests encompassed a variety of unbraced lengths and support conditions with steel diaphragms or timber ties acting as bracing members. The interior beam in the test assembly was loaded orthogonal to its strong axis at the middle of one or both spans using a spreader beam system that minimized restraint and prevented development of follower forces.

Test Setup

The test assembly was designed to address critical parameters from a group of representative bridges, including span, spacing, stringer size, material properties, and support conditions. The test assembly also accommodated a variety of bracing configurations, stringer-to-floor beam relative stiffness, and connection fixity conditions. The test assembly included three lines of 50-ft-long W16×31 stringers, one 25-ft-long W24×68 floor beam, and C12×20 end diaphragms bolted to the stringers. Figures 2 and 3 show the framing plan and a section at the floor beam, respectively. Stringer center-to-center span lengths were 24 ft. The floor beam was supported by interior steel bearing plates at the stringer locations to represent a rigid support (neglect floor beam displacements). Without these interior plates, the floor beam was free to bend between its end supports, thereby representing flexible supports for the stringers. Additionally, the stringer bottom flange was bolted or unbolted to the floor beam to simulate various fixity conditions. The bolted condition provided resistance to slippage and anchored the bottom flange to the floor beam, thereby providing rotational (i.e., torsional) resistance. Without the bolts, the floor beam acted as a vertical bearing support, and any translational resistance was provided by friction that might occur between the stringer and floor beam flanges. The stringer bottom flange was also free to uplift from the floor beam flange due to torsion.

Grade 50 W16×31 sections were selected for the stringers because they represent stringers used on Louisiana bridges. They also were expected to exhibit elastic LTB behavior, which allowed for repetitive tests. Furthermore, Gr. 50 yield strengths vary less than Gr. 36, and steel grade minimally impacts controlling L_b or L_r.

Test Matrix

Table 1 provides the test matrix, including test groupings, corresponding configurations (i.e., test setups), stringer support conditions (i.e., floor beam flexural stiffness), loading and bracing conditions, and assigned test identification numbers. The experimental program included test setups with and without a noncomposite concrete deck. This paper addresses the tests without the deck, which are categorized into three general groups. A concentrated force was applied at midspan of one or both spans for balanced and unbalanced loading conditions, respectively.

A balanced load referred to a load case in which both spans of the interior stringer were loaded at midspan. An unbalanced load meant that one span of the interior stringer was loaded at midspan. For illustration purposes, Figure 4 shows one- and two-point loads at midspan of the interior stringer, and corresponding moment diagrams are illustrated in Figure 5. When an unbalanced load was applied, the unloaded stringer end was tied to the strong floor to avoid uplift. Stringer geometry measurements were collected using laser scans prior to the tests. The maximum

Fig. 1. I-10 Mississippi River Bridge in Port Allen, La. (photo courtesy of Suba Herath).

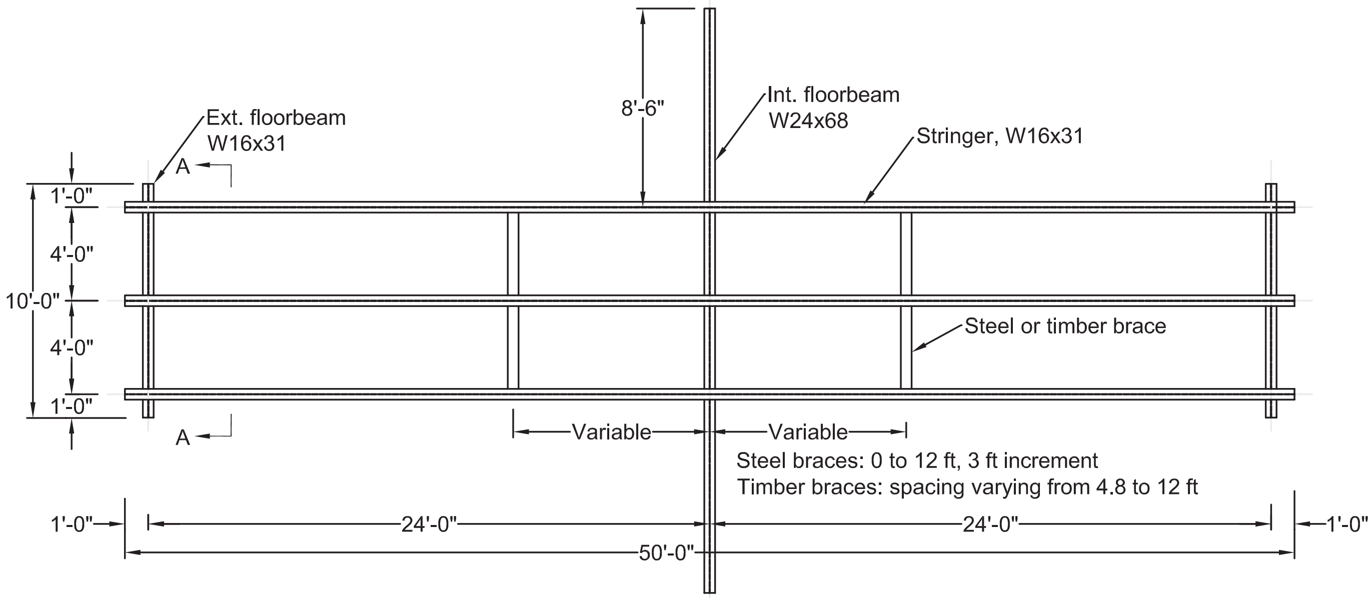

Fig. 2. Test assembly framing plan.

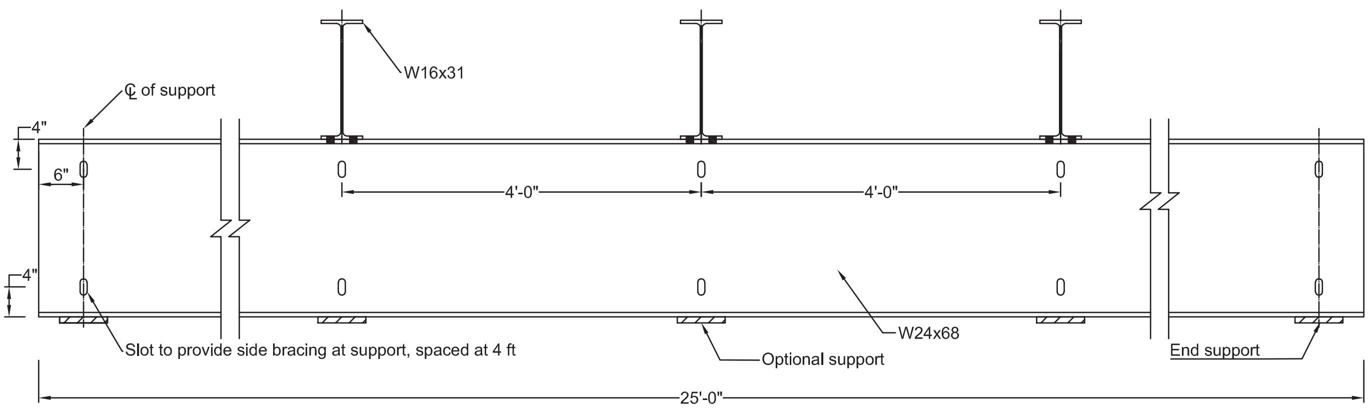

Fig. 3. Test assembly section at floor beam.

Table 1. Test Matrix					
	Description of Boundary Conditions				
Group	Interior Support at Center Stringer	Top Flange of Stringer	Stringer Bottom Flange to Floor Beam Connection	Load Condition	Test No.
I	Rigid	Unbraced	Unbolted to floor beam	1 point load	1
				2 point loads	2
			Bolted to floor beam	1 point load	3
				2 point loads	4
	Flexible		Unbolted to floor beam	1 point load	5
				2 point loads	6
			Bolted to floor beam	1 point load	7
				2 point loads	8
II	Rigid	Diaphragms at interior support	Unbolted to floor beam	1 point load	9
				2 point loads	10
		Diaphragms at *L*/2		1 point load	11
				2 point loads	12
		Diaphragms at *L*/8 from interior support		1 point load	13
				2 point loads	14
		Diaphragms at *L*/4 from interior support		1 point load	15
				2 point loads	16
		Diaphragms at 3*L*/8 from interior support		1 point load	17
				2 point loads	18
	Rigid	Diaphragms at interior support	Bolted to floor beam	1 point load	19
				2 point loads	20
		Diaphragms at *L*/2		1 point load	21
				2 point loads	22
		Diaphragms at *L*/8 from interior support		1 point load	23
				2 point loads	24
		Diaphragms at *L*/4 from interior support		1 point load	25
				2 point loads	26
		Diaphragms at 3*L*/8 from interior support		1 point load	27
				2 point loads	28

(table continued on next page)

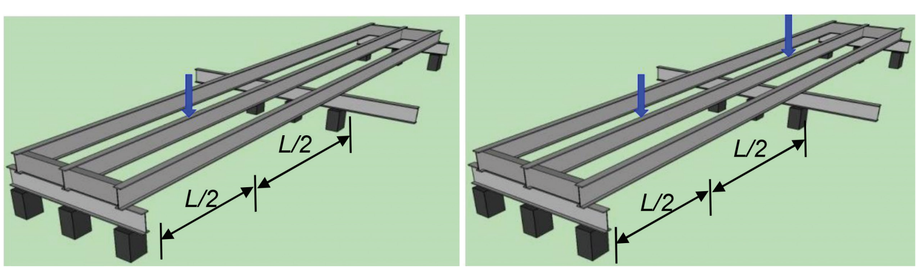

(a) Unbalanced load *(b) Balanced load*

Fig. 4. Load conditions.

Table 1. Test Matrix (continued)					
Group	Description of Boundary Conditions: Interior Support at Center Stringer	Description of Boundary Conditions: Top Flange of Stringer	Description of Boundary Conditions: Stringer Bottom Flange to Floor Beam Connection	Load Condition	Test No.
III	Rigid	Timber ties at *L*/2	Unbolted to floor beam	2 point loads	29
		Timber ties at *L*/3			30
		Timber ties at *L*/4, *L*/2, *L*, *L*/2, *L*/4			30'
		Timber ties at *L*/4			31
		Timber ties at *L*/5			32
		Timber ties at *L*/2	Bolted to floor beam	2 point loads	33
		Timber ties at *L*/3			34
		Timber ties at *L*/4, *L*/2, *L*, *L*/2, *L*/4			34'
		Timber ties at *L*/4			35
		Timber ties at *L*/5			36
		Timber ties at *L*/8, *L*/4, *L*/2, L, *L*/8, L/4, L/2			36'
	Flexible	Timber ties at *L*/2	Unbolted to floor beam	2 point loads	37
		Timber ties at *L*/3			38
		Timber ties at *L*/4			39
		Timber ties at *L*/5			40
		Timber ties at *L*/2	Bolted to floor beam	2 point loads	41
		Timber ties at *L*/3			42
		Timber ties at *L*/4			43
		Timber ties at *L*/5			44

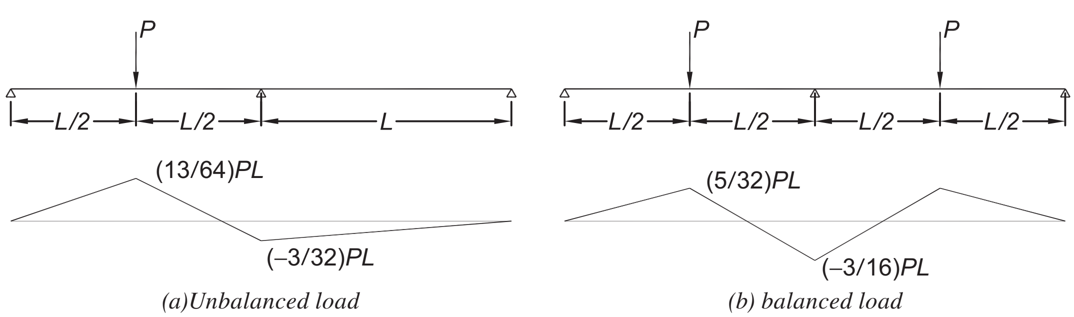

Fig. 5. Moment diagrams for two-span stringer.

sweep imperfection was approximately $L/1500$ (L = span) for the top flange at midspan.

Group I included Tests 1 to 8, in which the stringer top flanges were unbraced (Figure 6). Either a rigid or flexible interior floor beam supported the stringers. A rigid interior support was provided beneath the stringers by supporting the floor beam on the laboratory strong floor along its length using steel plates. Stringer bottom flanges were either unbolted or bolted to the floor beam. When bolted, four $\frac{7}{8}$-in.-diameter high-strength bolts were used. No stringer stiffeners were provided over the floor beam. Group I tests served as a baseline for comparison to other tests.

As shown in Figure 7, the load application system included upper and lower bearing plates with a spherical bearing between them. A load cell was installed between the upper plate and spreader beam to monitor the applied loads. A lubricant was applied to the spherical bearing to minimize friction between the spherical bearing and plates. As a result, rotational and lateral restraints from the load point were minimized. In addition, potential bracing

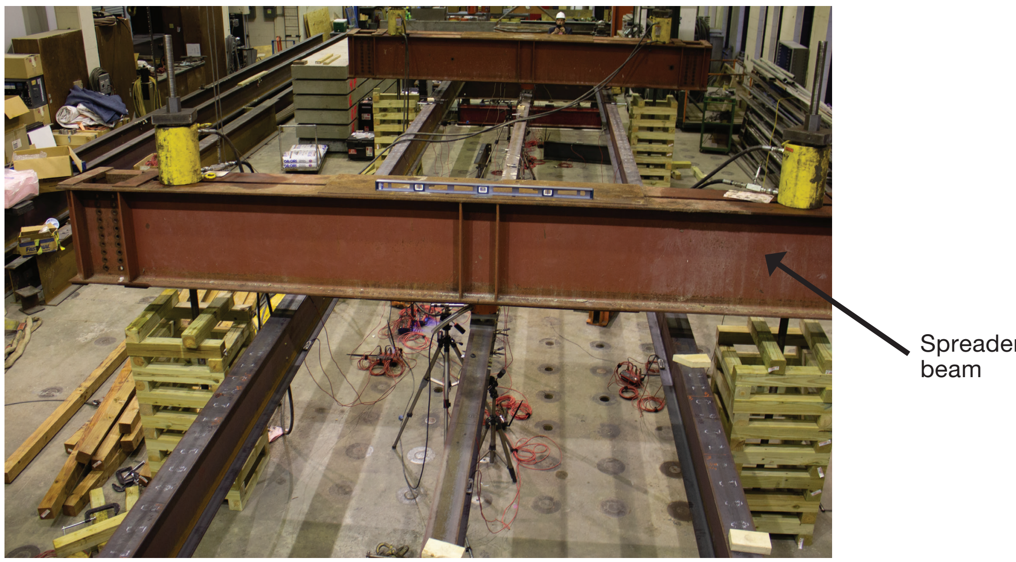

Fig. 6. Example Group I setup.

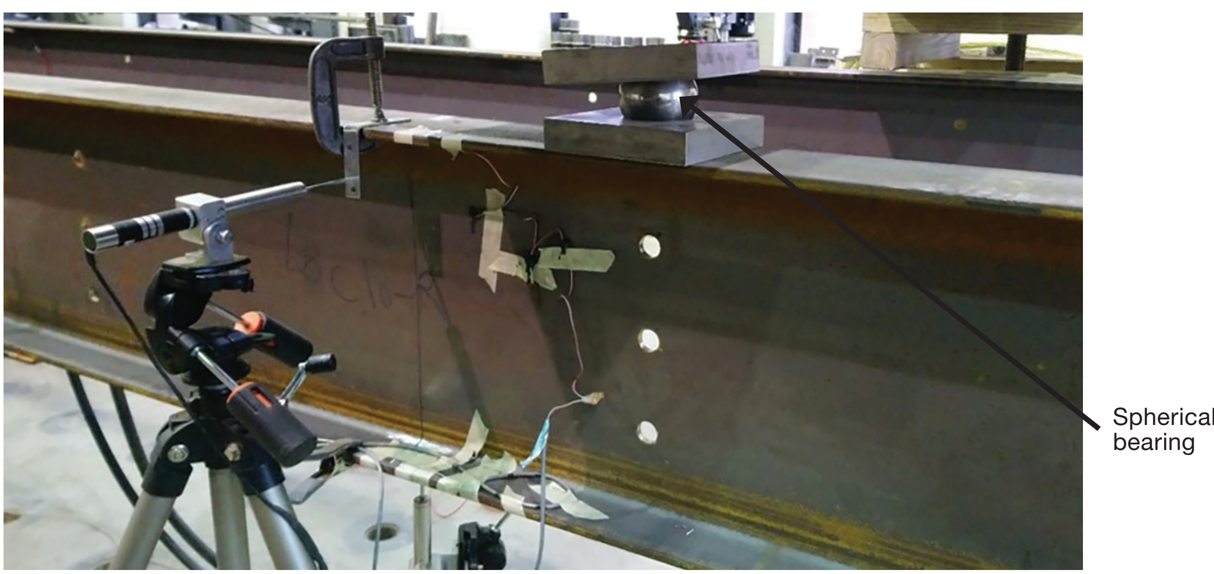

Fig. 7. Load application detail.

restraint from the spreader beams used to apply point loads was minimal because the spreader beam above the load cell was supported at its ends by two vertical threaded rods, whose flexural stiffness was measured and shown to be negligible.

Group II included Tests 9 to 28, where the stringers were braced by intermediate steel diaphragms at various locations, including the interior support and $L/2$, $L/8$, $L/4$, and $3L/8$ away from the interior support, where L is the span length. Diaphragms were bolted to the stringers, and the floor beam was supported along its length by the laboratory strong floor. Again, the stringer bottom flanges were either unbolted or bolted to the floor beam, and balanced and unbalanced loads were applied. Figure 8 depicts a representative Group II test.

Group III included Tests 29 to 44, in which the stringer top flanges were laterally braced using #2 red pine timber ties (4 in. × 4 in.) connected using C-clamps (Figure 9). Lateral support included a range of bracing locations before a noncomposite concrete deck was placed and allowed for a wide range of lateral support conditions to be efficiently studied. Consistent with the other groups, rigid or flexible interior floor beam support was provided, and stringer bottom flanges were either unbolted or bolted to the floor beam. Balanced loads were applied.

Instrumentation

Load and pressure cells, strain gages and transducers, and linear variable differential transformers (LVDTs) measured applied forces and structural response. Instrument locations are detailed in Figure 10. Strain gages and transducers were placed at multiple sections on the interior stringer and transducers at critical exterior stringer sections to capture effects due to primary, weak-axis, and lateral bending moments, as well as axial loads. Transducers were installed on both the top and bottom flanges. LVDTs were placed at midspan of the interior stringer in both spans and were oriented to capture vertical and lateral deflections. Load and pressure cells were provided at the spreader beams to apply load. Results were commonly reported at four critical locations as described in Table 2. Figures 11 and 12 detail LVDTs, strain gages, and transducers at Locations 10 and 4 (see Figure 10), respectively.

Test Results

Test results for Group I and III are provided herein. Representative results are presented as plots of applied load versus stringer vertical and lateral deflections, and load versus stringer strains. Applied load versus axial, and lateral, primary, out-of-plane, bending normal stress components are

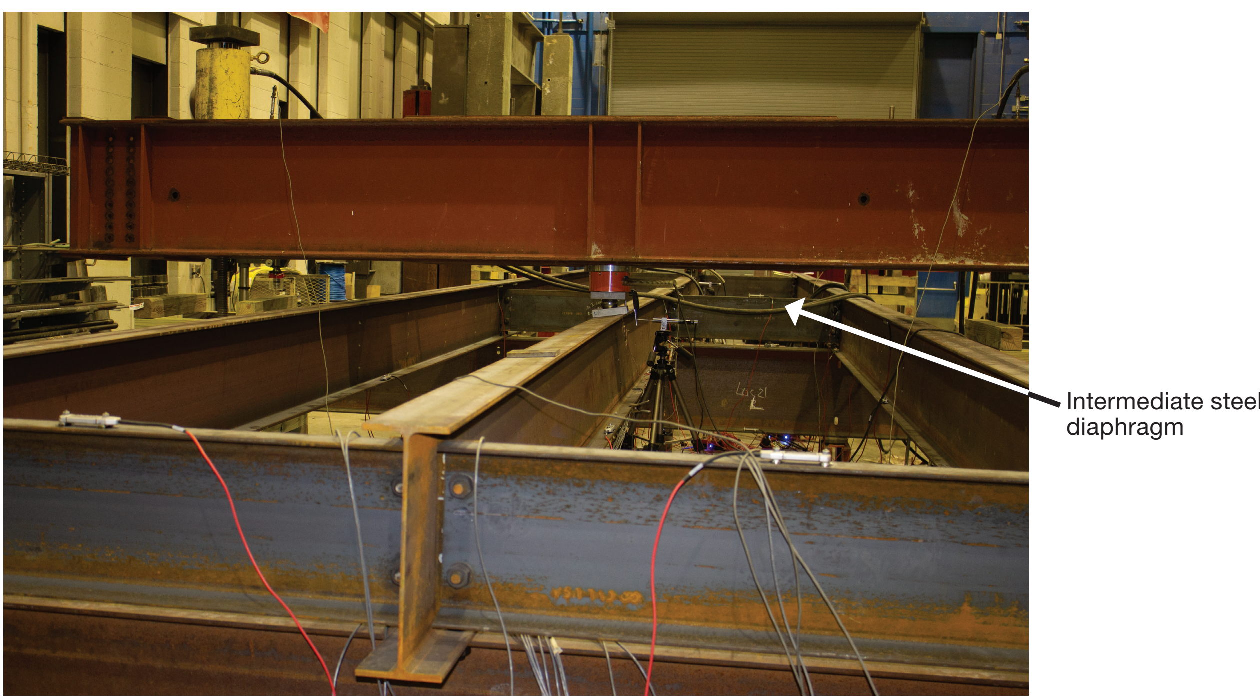

Fig. 8. Example Group II setup.

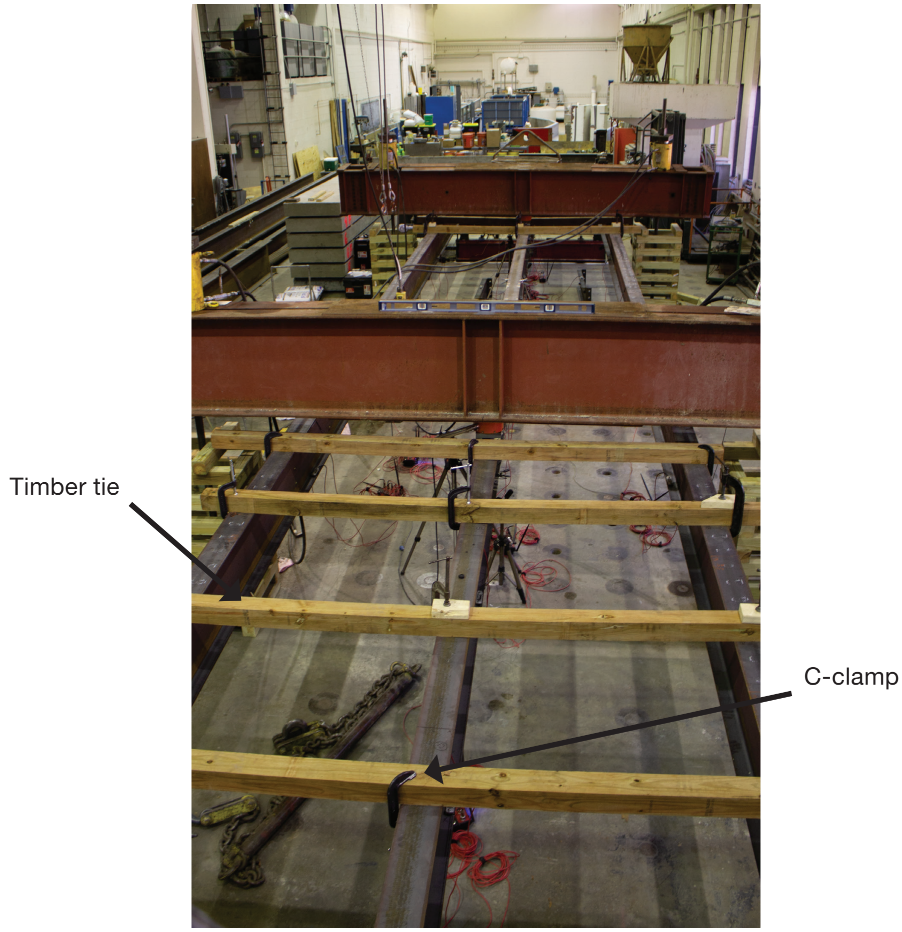

Fig. 9. Example Group III setup.

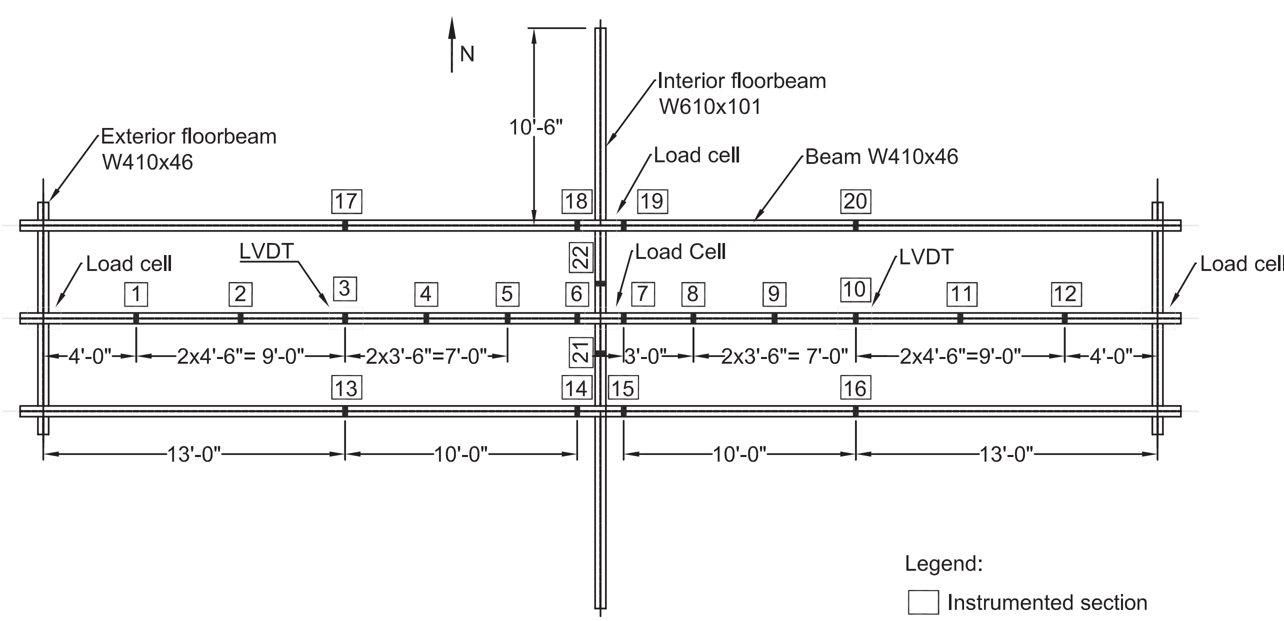

Fig. 10. Instrumentation plan view.

Table 2. Critical Locations	
Location	**Description**
3	Midspan maximum + M when loaded at Location 3 Midspan – M when loaded at Location 10 (see Figure 6)
6	Critical – M location adjacent to floor beam
7	Critical – M location adjacent to floor beam
10	Midspan maximum + M when loaded at Location 10 Midspan – M when loaded at Location 3 (see Figure 6)

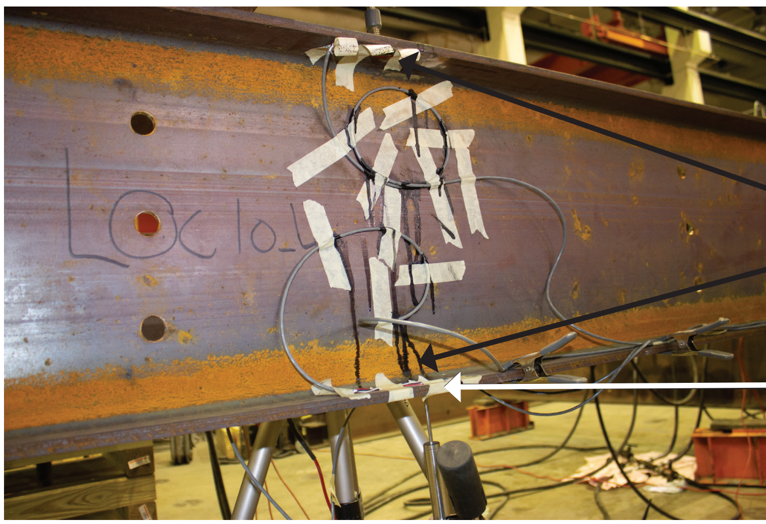

Fig. 11. LVDT and strain transducers, Location 10.

Fig. 12. Strain gage, Location 4.

Gauge		One Spreader Beam (Unbalanced Load)			Two Spreader Beams (Balanced Load)		
		Measured Stress (ksi)	Predicted Stress (ksi)	Ratio	Measured Stress (ksi)	Predicted Stress (ksi)	Ratio
Ch0	Top	1.04	1.15	90%	–2.58	–2.96	87%
Ch1	Bottom	–0.98	–1.15	85%	3.03	2.96	103%
Ch2	Bottom	–0.98	–1.15	85%	2.71	2.96	92%

Table 3. Test and Elastic Analysis Stresses, Spreader Beam Placement

also provided. More complete data are provided in Sun et al. (2021).

Group I Tests—Unbraced

As indicated in Table 1, Group I tests had no intermediate bracing. Figure 13 depicts Test No. 3, showing vertical and lateral LVDTs on the interior stringer, the spreader beam, and corresponding load cell at midspan, a supported floor beam, and the bolted connection between the interior stringer and floor beam.

Each spreader beam weighed approximately 3.7 kips. For tests that had loads applied at midspan of both spans, data were recorded as the spreader beams were sequentially placed onto the test assembly and measured deflections caused by their placement compared well with elastic analyses. Corresponding measured, midspan stresses from strain data were comparable to calculated stresses as shown in Table 3.

Tests 1, 3, 5, and 7 results are presented for discussion purposes because they experienced LTB and accounted for various support and bracing conditions: a rigid or flexible interior floor beam with the stringer bottom flanges either unbolted or bolted to the floor beam. Load-lateral deflection plots in Figure 14 show that Test No. 3 provided the largest lateral stiffness because stringer bottom flanges were bolted to the floor beam and the interior support was considered rigid (i.e., floor beam supported along its length). There is apparent noise in the plots in Figure 14 because tests were run in force control and applied loads were manually controlled, resulting in some relaxation of the system after each load step. Figure 15 depicts the LTB of the interior stringer for Test No. 3. Test No. 1 exhibited the highest lateral flexibility because stringer bottom flanges were not bolted to the floor beam. Tests 5 and 7, both of which had flexible interior supports and unbolted and bolted stringer flanges, exhibited lateral stiffness between Tests 1 and 3. Test No. 7 provided slightly higher lateral stiffness than Test No. 5 because stringer bottom flanges were bolted to the floor beam.

Figures 16 and 17 present load-strain plots for transducers at Location 3 TN (top north) and TS (top south) for the four tests. Figure 18 identifies transducer locations. Test No. 1 exhibited comparable strains to the other three tests until it reached peak load, which, again, was lower than that for the other tests. LTB was evident via measured bifurcation for three of the four tests.

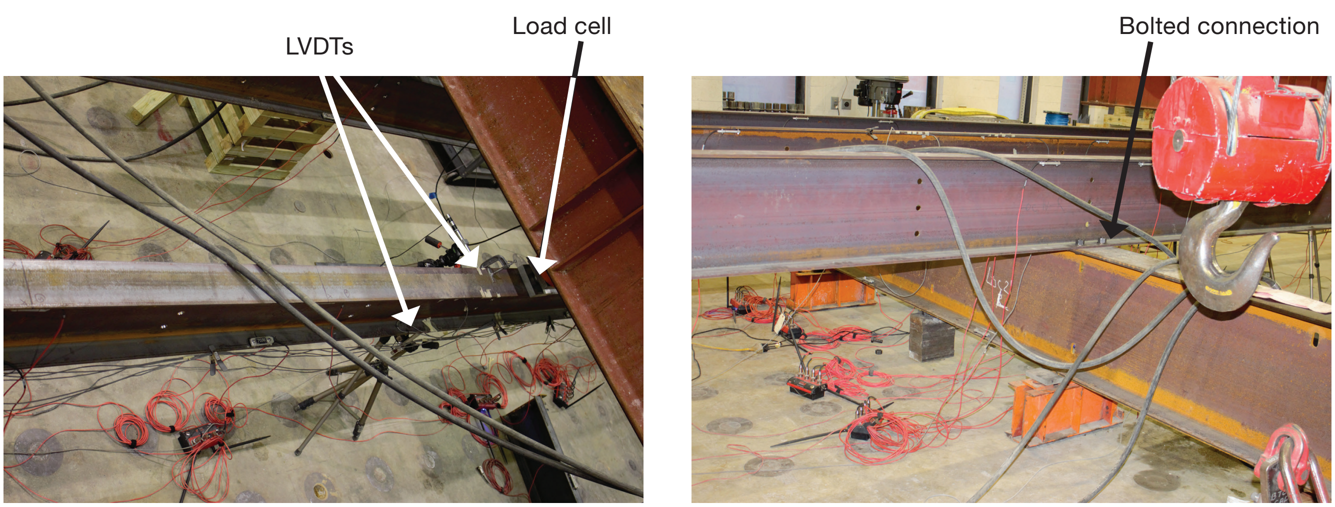

(a) Midspan LVDTs and load cell

(b) Supports and bolted connection at floor beam

Fig. 13. Test No. 3.

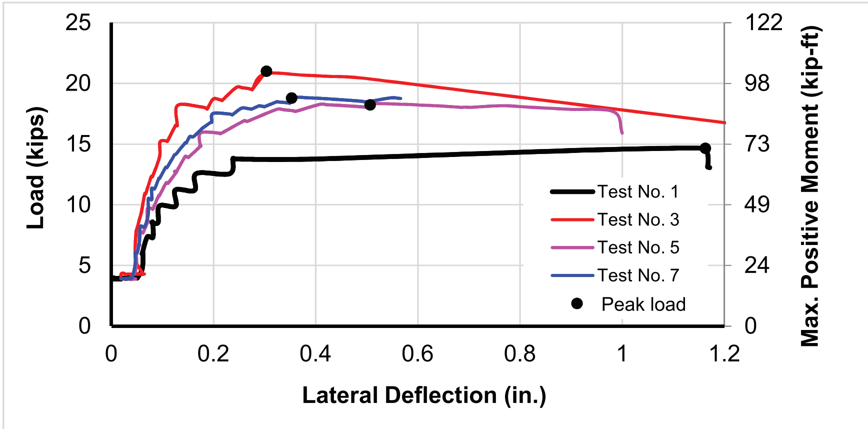

Fig. 14. Load versus lateral deflections, Tests 1, 3, 5, and 7.

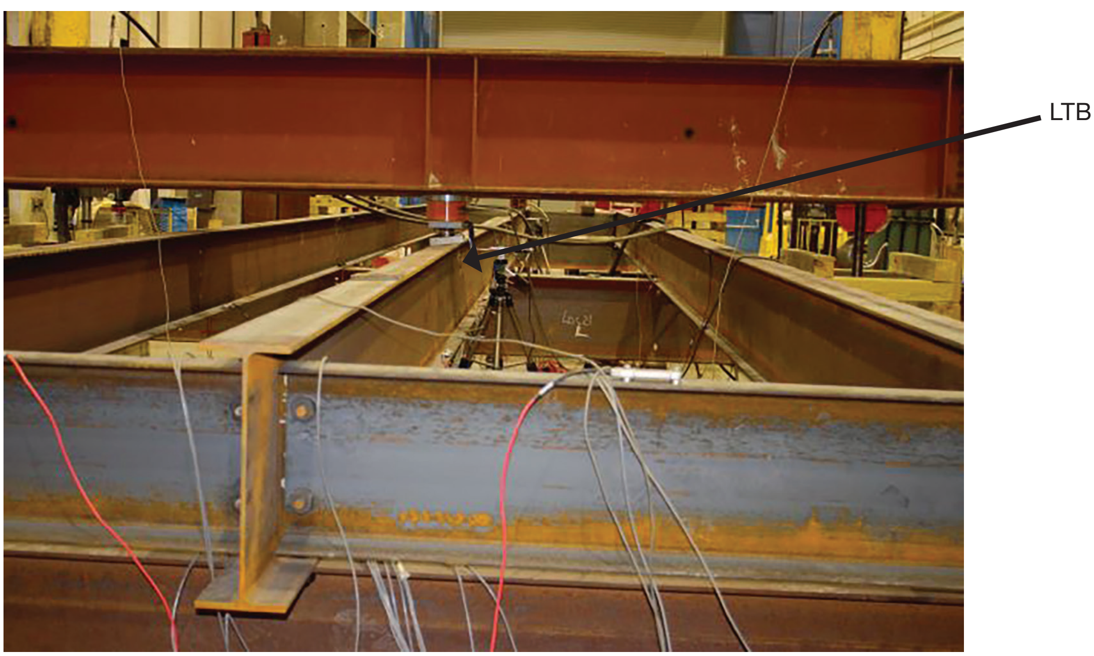

Fig. 15. LTB of the interior stringer, Test No. 3.

To further assess behavior at a typical section, strains were converted to stresses and values were decoupled to capture axial (σ_a), and primary (σ_x), out-of-plane (σ_y), and lateral bending (σ_w) normal stress components. Equations 1 through 4 detail relationships between total stress and its components at each of the four instrument locations in a typical cross section (i.e., TN, TS, BN, and BS in Figure 18).

$$f_{TN} = -\sigma_x + \sigma_y - \sigma_w + \sigma_a \tag{1}$$

$$f_{TS} = -\sigma_x - \sigma_y + \sigma_w + \sigma_a \tag{2}$$

$$f_{BN} = \sigma_x + \sigma_y + \sigma_w + \sigma_a \tag{3}$$

$$f_{BS} = \sigma_x - \sigma_y - \sigma_w + \sigma_a \tag{4}$$

For illustrative purposes, Figure 19 shows stress components at Location 3 TN for Test No. 1. As expected, the axial stress was zero, while weak-axis and lateral bending stresses shown in Figures 19 through 22 experienced a gradual increase after peak load, indicating LTB. As shown in Figures 19 and 20, the magnitude and sign associated with top of flange out-of-plane and lateral bending stresses influenced total stress. Figures 21 and 22, which plot bottom flange stress components, indicate that out-of-plane and lateral bending stresses were of opposite sign and did not significantly affect total stress.

Figure 23 illustrates the effect of floor beam relative stiffness on observed response for Tests 1 to 8. For most cases, a flexible floor beam resulted in an appreciable difference in LTB resistance, with peak loads changing by more than 25%. Negative moments decreased due to translation of the floor beam. Figure 24 illustrates the effect of the stringer-to-floor beam fixity for Tests 1 to 8. LTB commonly occurred at higher applied loads when the stringer bottom flange was connected to the floor beam because of increased lateral restraint. Stringer bracing conditions over the floor beam were established to represent continuous stringers in Louisiana bridges. As stated earlier, Group I tests served as comparison baselines for the additional non-composite tests (Sun et al., 2022). As a result, a diaphragm

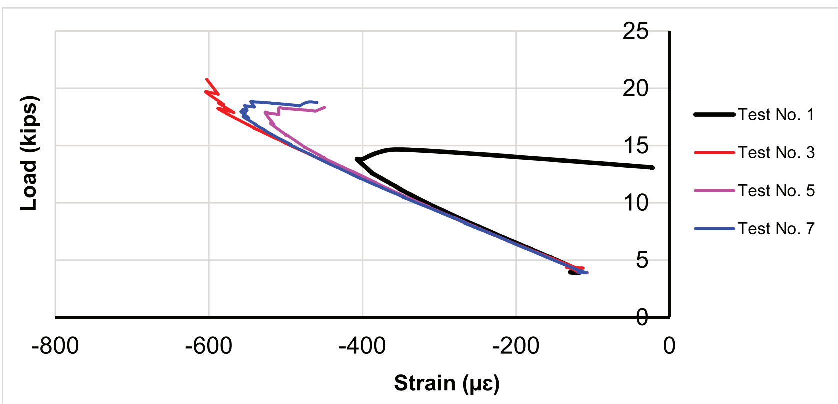

Fig. 16. Load-strain plots at Location 3 TN, Tests 1, 3, 5, and 7.

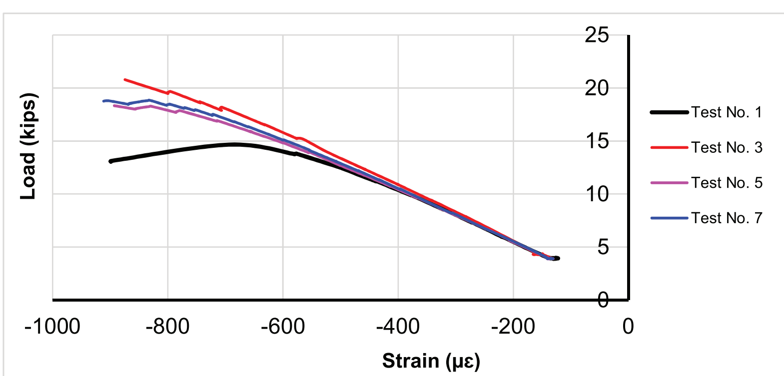

Fig. 17. Load-strain plots at Location 3 TS, Tests 1, 3, 5, and 7.

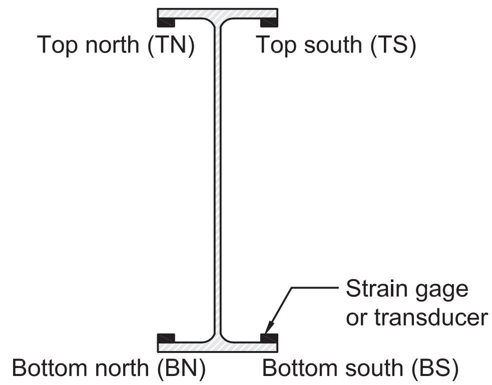

Fig. 18. Strain transducer locations.

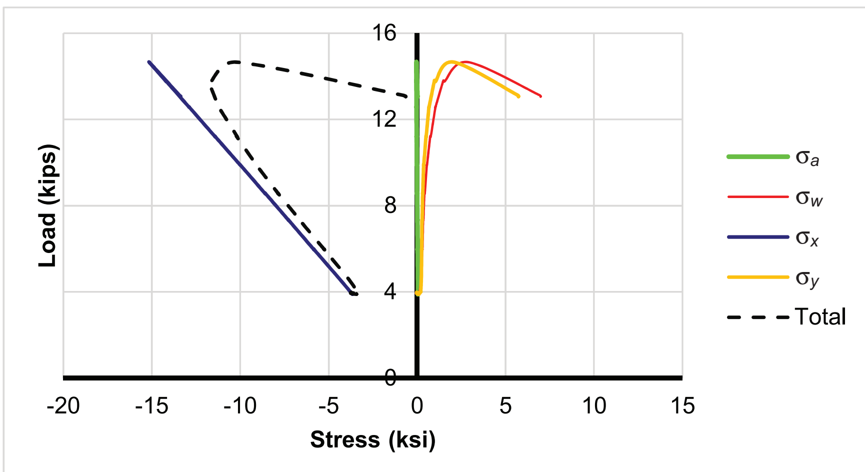

Fig. 19. Stress components, Location 3 TN, Test No. 1.

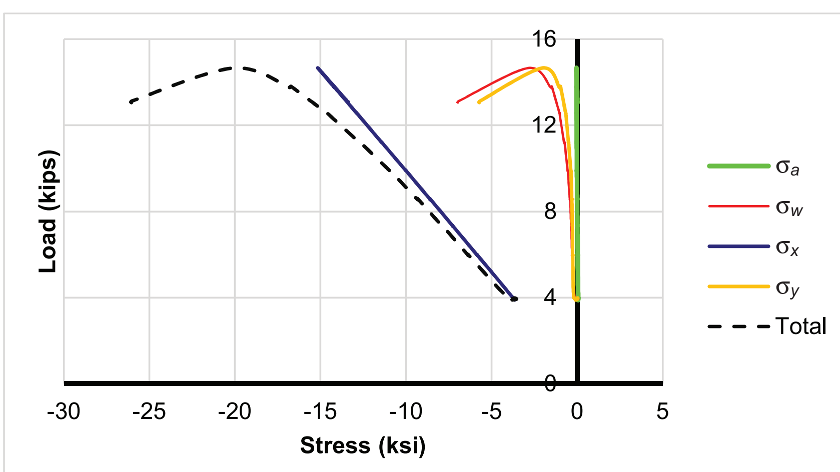

Fig. 20. Stress components, Location 3 TS, Test No. 1.

was not provided between adjacent stringers over the floor beam for Test 1 to 8. Those tests that included unbolted stringer bottom flanges helped evaluate LTB resistance for situations where the unbraced length did not explicitly meet the formal definition for unbraced length in LTB equations used in current codes and specifications. It was observed that stringer compression flanges at both supports should be laterally braced.

Group II Test Results—Intermediately Braced by Diaphragms

Intermediate steel diaphragms were installed at various locations for Group II tests to determine their effect on LTB. Rigid interior supports were provided, and stringer bottom flanges were either unbolted or bolted at the floor beam using ⅞-in.-diameter high-strength bolts. The interior stringer was loaded at midspan of one or both spans. The unbraced lengths varied from 12 to 24 ft. The longer unbraced lengths corresponded to reduced buckling loads, as expected. The connection types (e.g., bolted or unbolted connections) at the stringer bottom flange affected the buckling load, with unbolted connections generally resulted in a slightly lower buckling load. Refer to Sun et al. (2021) for more detailed discussion of these tests.

Group III Test Results—Intermediate Bracing Using Timber Ties

As indicated in Table 1, Group III tests were of stringers braced using 4 in. × 4 in. timber ties, which were affixed to the stringer top flanges using C-clamps. As stated earlier,

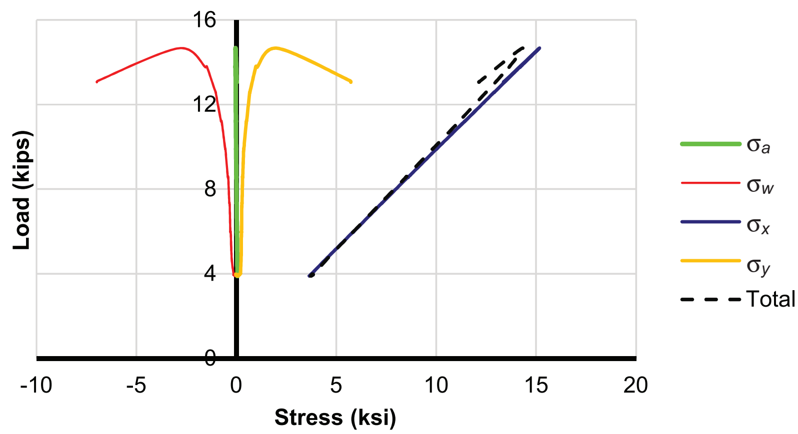

Fig. 21. Stress components, Location 3 BN, Test No. 1.

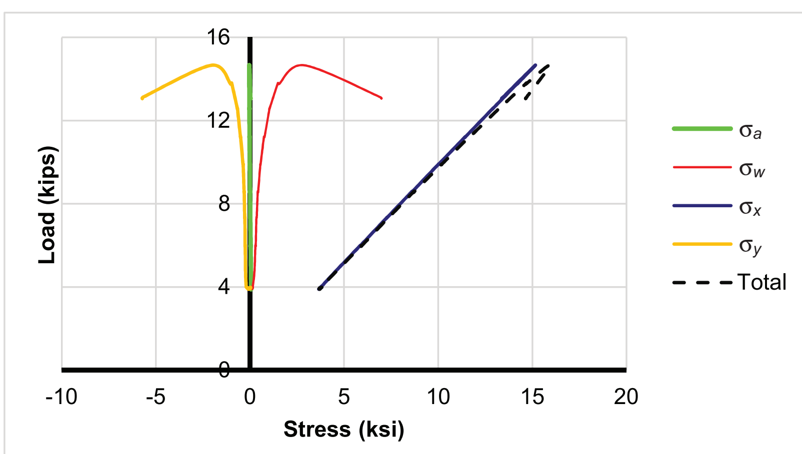

Fig. 22. Stress components, Location 3 BS, Test No. 1.

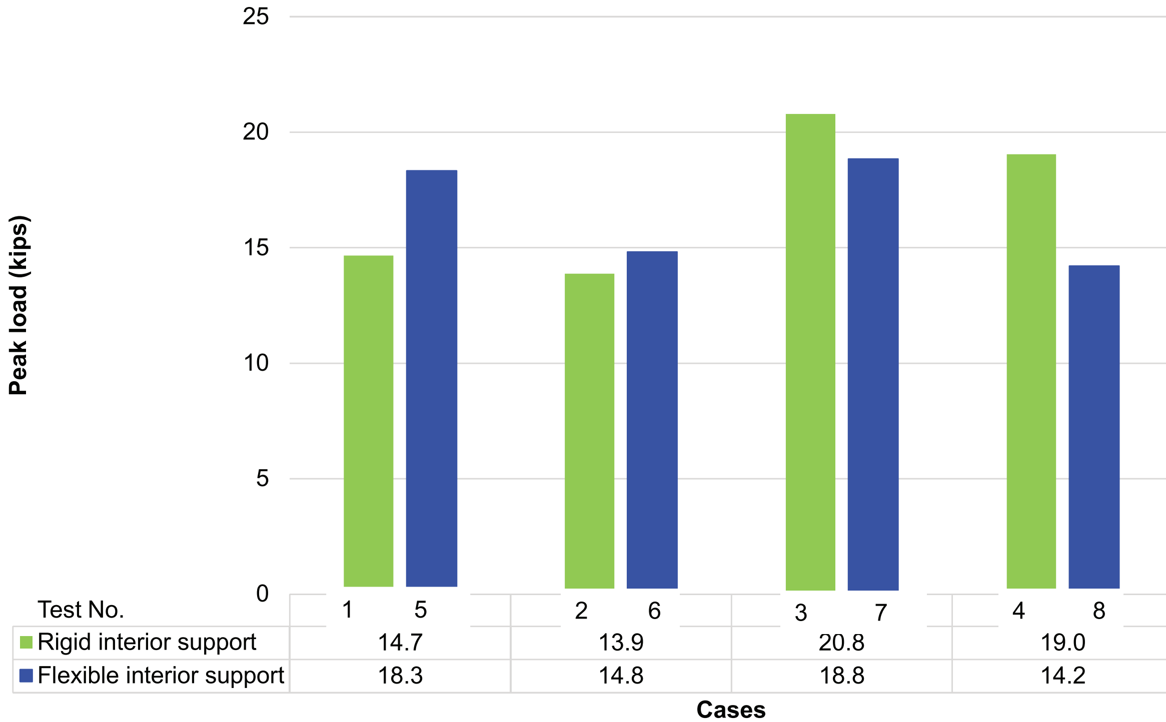

Fig. 23. Effect of floor beam relative stiffness on loading capacity.

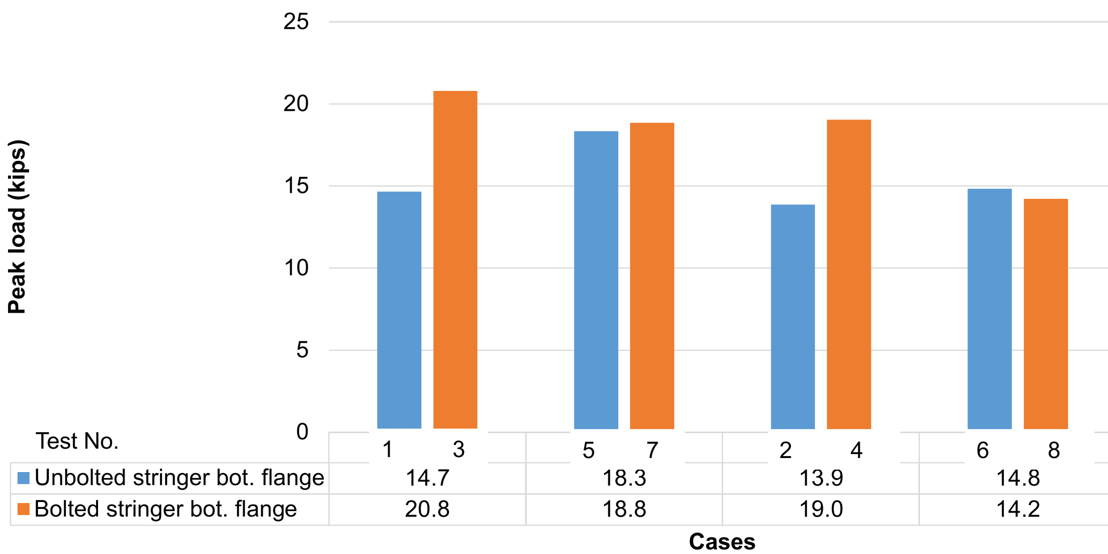

Fig. 24. Effect of stringer to floor beam fixity on loading capacity.

these tests were completed to demonstrate that a small increase in bracing, even with low strength, can significantly change LTB behavior. Table 4 provides descriptions of Tests 2 and 29 to 32, which were subjected to concentrated loads at midspan of both spans. Figure 25 plots load versus lateral deflection, and Figure 26 plots load versus strain at Location 3 TN. Beneficial effects provided by minimal lateral bracing, ones that increase LTB resistance, are clearly demonstrated via placement of a pair of timber ties at midspan (Test No. 29), which nearly doubled the capacity compared to the baseline unbraced test (Test No. 2). Midspan bracing was also more effective than bracing using ties spaced at $L/3$ (Test No. 30). Bracing effects for ties spaced at $L/4$ and $L/5$ (Tests 31 and 32) were nearly identical and only nominally improved capacity over that observed for Test No. 29. These findings were generally consistent with those from full-scale tests of a timber deck conducted by Webb and Yura (1992), in which the friction between the deck and stringer was shown to increase strength. A full-size test on a five-beam, short, single-span bridge conducted by Vegesna and Yura (1992) also showed that timber decks not positively attached to supporting stringers doubled stringer LTB resistance.

The level of lateral restraint provided by minimal placement of timber ties [i.e., small bracing stiffness and connection strength (C-clamps)] was further evaluated for several tests having either rigid or flexible interior supports. Results are shown in Figures 27 and 28. These figures plot peak loads as a function of tie spacing and compare them to baseline tests (e.g., Tests 2, 4, 6, and 8) where no ties

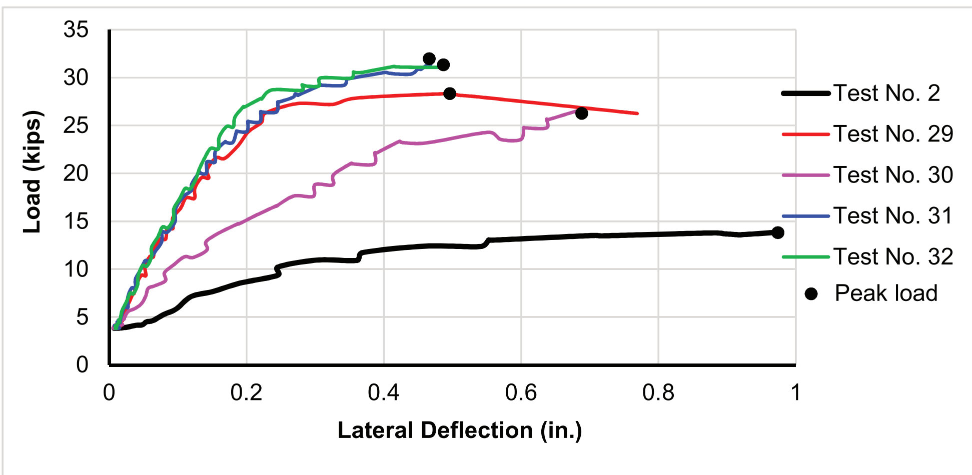

Fig. 25. Load versus lateral deflections, Tests 2 and 29 to 32.

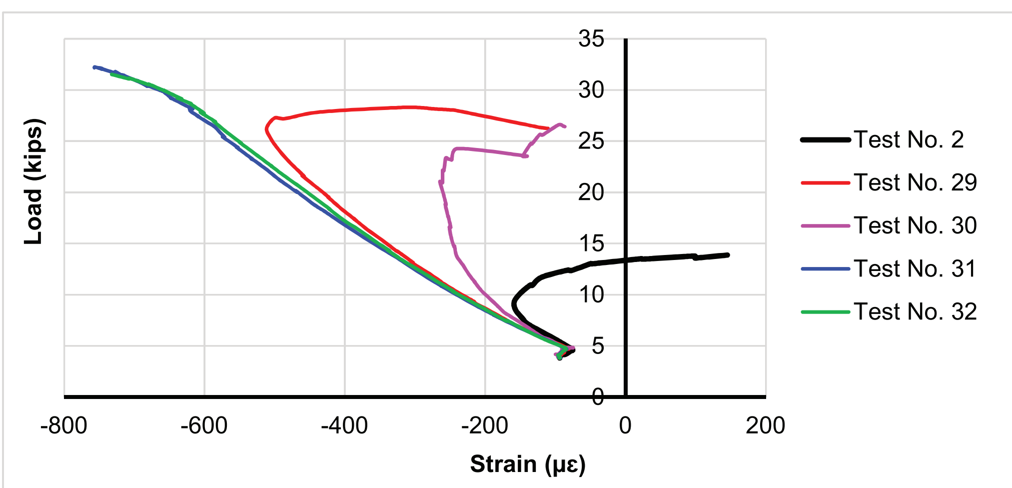

Fig. 26. Load-strain plots at Location 3 TN, Tests 2 and 29 to 32.

Table 4. Descriptions of Tests 2 and 29 to 32, Both Spans Loaded

Test No.	Boundary Conditions: Floor Beam Relative Stiffness	Boundary Conditions: Stringer Top Flange Bracing		Boundary Conditions: Stringer Bottom Flange to Floor Beam Connection
2	Rigid	Unbraced		Unbolted to floor beam
29	Rigid	Timber ties (4 in. × 4 in.), connected using C-clamps	Spaced at $L/2$	Unbolted to floor beam
30			Spaced at $L/3$	
31			Spaced at $L/4$	
32			Spaced at $L/5$	

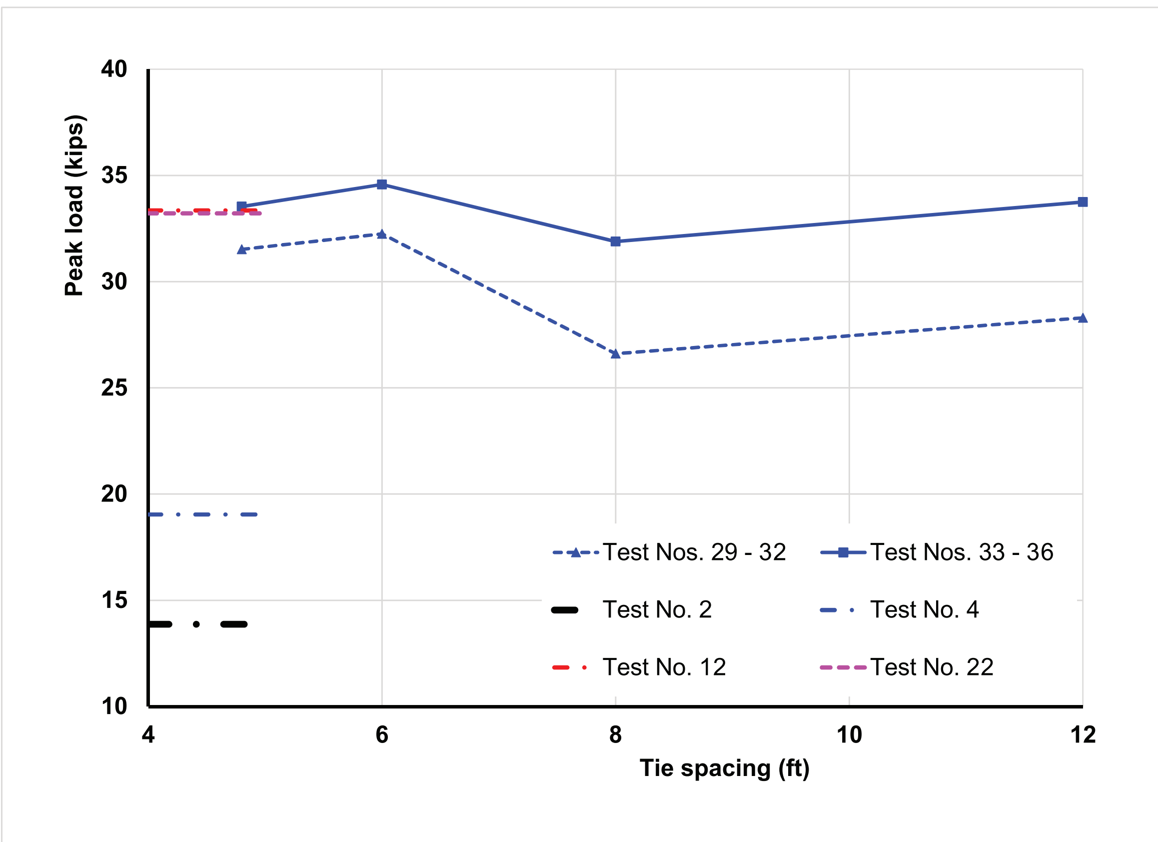

Fig. 27. Timber tie bracing effects, rigid interior support.

were provided. Figure 27 also shows peak loads for Tests 12 and 22, which had steel diagrams installed at midspan. The bracing effect provided by the timber ties at spacings of Span/4 and Span/5 was comparable to that of the steel diaphragms at midspan. Group III tests show that LTB resistance can be increased significantly using minimal lateral stiffness provided by C-clamped 4 in. × 4 in. timber ties and lend credence to potential LTB resistance noncomposite decks can provide.

CONCLUSIONS

An experimental study was completed to examine LTB resistance of continuous stringers. The assembly was designed to represent floor systems in twin girder or truss bridges in Louisiana and was subjected to loads that represented design tandems or design trucks. The study outlined herein was part of a larger study that included a noncomposite, cast-in-place concrete deck. It included extensive tests of a two-span test assembly containing three stringer lines and a supporting floor beam. A variety of unbraced lengths and stiffness were investigated along with flexible and rigid interior supports, and bolted and unbolted connections between the stringer bottom flange and interior supporting floor beam. Both steel diaphragms and timber ties acted as bracing members. Results provided a robust database for evaluation of continuous beam LTB resistance. The following conclusions were drawn:

1. A flexible interior support (i.e., floor beam) largely produced LTB resistances that differed by 25% from rigid interior support cases.
2. LTB commonly occurred at higher applied loads when the stringer bottom flange was bolted to its supporting floor beam.
3. Minimal lateral bracing stiffness provided by 4 in. by 4 in. timber ties and C-clamps provided benefit to stringer LTB resistance, with capacities nearly doubling compared to baseline, unbraced tests. These results appear to justify higher LTB resistances than what are typically used for noncomposite concrete decks.

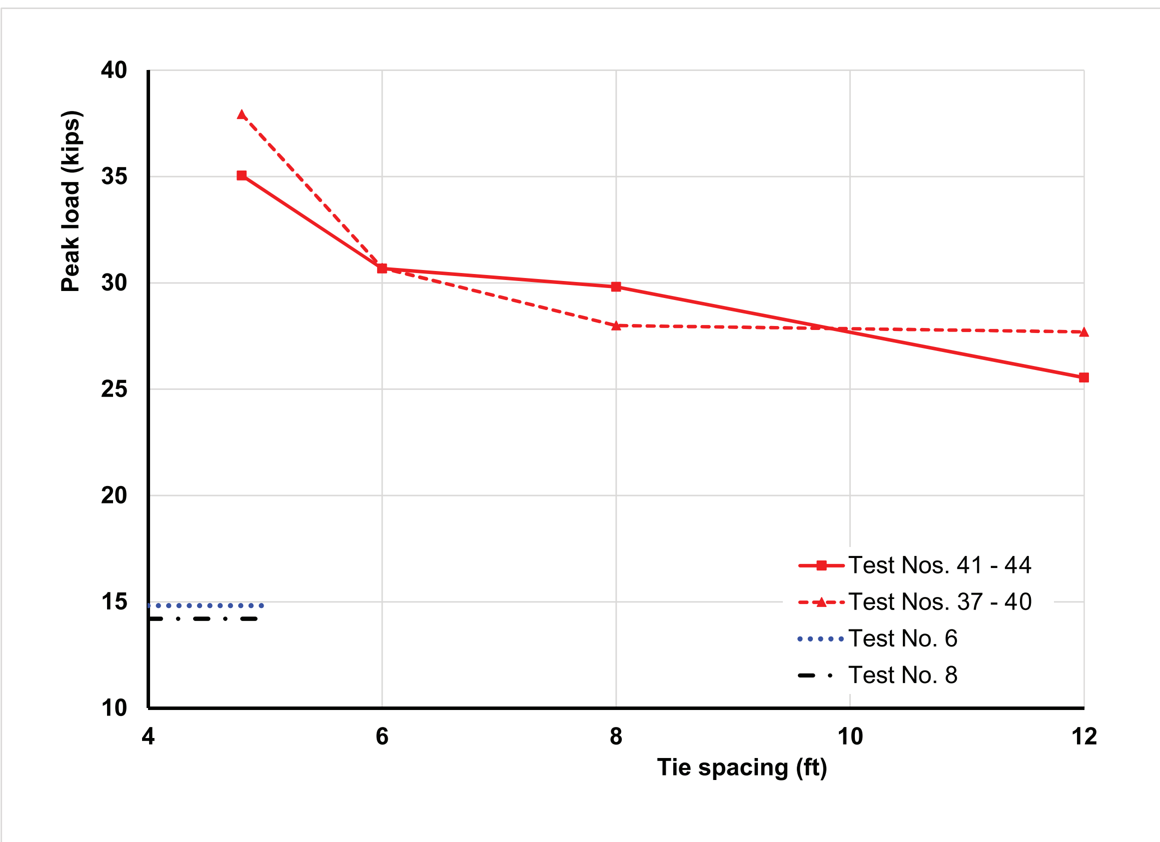

Fig. 28. Timber tie bracing effects, flexible interior support.

ACKNOWLEDGMENTS

The authors would like to thank the LTRC and the LA DOTD for funding this project. The authors are grateful to the Project Review Committee Members, including Art Aguirre, Alden Allen, Michael Boudreaux, Mark Bucci, Nick Fagerburg, Dana Feng, Kelly Kemp, William Metcalf, and Kian Yap, for their guidance and support. Special thanks go to Walid R. Alaywan, Senior Structures Research Engineer at the LTRC, for leading and managing this project. The authors are also grateful to Peter Hilsabeck for assisting in lab testing. The contents of this paper do not necessarily reflect the official views or policies of the LA DOTD and LTRC.

REFERENCES

AASHTO (2020), *AASHTO LRFD Bridge Design Specifications*, 9th Ed., American Association of State Highway and Transportation Officials, Washington, D.C.

Sun, C., Linzell, D., and Puckett, J. (2021), "Load Rating of Existing Continuous Stringers on Louisiana's Bridges," LTRC Project 18-4ST Report, Louisiana Transportation Research Center, Baton Rouge, La.

Sun, C., Linzell, D., Puckett, J., Akintunde, E., and Rageh, A. (2022), "Experimental Study of Continuous Beam Lateral Torsional Buckling Resistance with a Noncomposite Concrete Deck," *Journal of Structural Engineering*, Vol. 148, No. 4, 04022026.

Vegesna, S. and Yura, J.A. (1992), "An Ultimate Load Test to Study Bracing Effects of Bridge Decks," Report No. FHWA/TX-92+1239-2, Center for Transportation Research, University of Texas at Austin, Austin, Texas.

Webb, S.T. and Yura, J.A. (1992), "Evaluation of Bridge Decks as Lateral Bracing for Supporting Steel Stringers," Report No. FHWA/TX-92+1239-3, Center for Transportation Research, University of Texas at Austin, Austin, Texas.